

## **Publisher Correction to: Even numbered carbon clusters: cost-effective wavefunction- based method for calculation and automated location of most structural isomers<sup>\*,\*\*</sup>**

**Eur. Phys. J. D (2018) 72: 134, <https://doi.org/10.1140/epjd/e2018-90145-4>**

António J.C. Varandas<sup>1,2,a</sup>

<sup>1</sup> School of Physics and Physical Engineering, Qufu Normal University, 273165 Qufu, P.R. China

<sup>2</sup> Chemistry Centre and Department of Chemistry, University of Coimbra, 3004-535 Coimbra, Portugal

Received 13 September 2018

Published online 16 October 2018

© EDP Sciences / Società Italiana di Fisica / Springer-Verlag GmbH Germany, part of Springer Nature, 2018

The figures were missing in the online version of the published article. This erratum provides the correct online file. The Publisher apologizes for the inconvenience.

\* The online version of the original article can be found at <https://doi.org/10.1140/epjd/e2018-90145-4>.

\*\* Contribution to the Topical Issue “Atomic Cluster Collisions”, edited by Alexey Verkhovtsev, Andrey V. Solov'yov, Germán Rojas-Lorenzo, and Jesús Rubayo Soneira.

<sup>a</sup> e-mail: [varandas@uc.pt](mailto:varandas@uc.pt)

# Even numbered carbon clusters: cost-effective wavefunction-based method for calculation and automated location of most structural isomers<sup>\*</sup>

António J.C. Varandas<sup>1,2,a</sup>

<sup>1</sup> School of Physics and Physical Engineering, Qufu Normal University, 273165 Qufu, P.R. China

<sup>2</sup> Chemistry Centre and Department of Chemistry, University of Coimbra, 3004-535 Coimbra, Portugal

Received 29 March 2018

Published online 2 August 2018

© EDP Sciences / Società Italiana di Fisica / Springer-Verlag GmbH Germany, part of Springer Nature, 2018

**Abstract.** Using second-order Möller-Plesset perturbation-theoretic calculations with extrapolation of the energy from the lowest steps of the hierarchical staircase to the complete basis set limit, a wave function-based approach emerges that rivals density functional theory in accuracy and cost-effectiveness. Tested on a large set of reactions, the method is now applied to the carbon clusters. Combined with variable-scaling opposite spin theory, the results approximate couple-cluster quality at no additional cost. Jointly with a stimulated breakup of the molecule by choosing a (simple or composite) driving coordinate at an adequate level of theory, the approach still offers a near automated tool for locating structural isomers along the optimized reaction coordinate for stimulated evolution so obtained. Adaptations are also suggested.

## 1 Introduction

Carbon clusters have long attracted both chemists and physicists alike for a number of reasons. The smaller play a key role in the chemistry of carbon rich stars, comets, and interstellar molecular clouds, while acting as building blocks in forming complex carbon-containing compounds. Added to this panoplia of astrophysical significance, they are of interest in connection with the formation of fullerenes, nanotubes, carbon-rich thin films, and the predominant species in terrestrial sooting flames; the bibliography is vast, with the reader addressed to a few papers [1–9] from which others may be obtained by cross-referencing. All the above finds justification on the exceptional bonding properties of carbon and its unique ability to form single, double, and triple (eventually quadruple in the dimer [10]) bonds. Naturally, elucidation of the possible mechanisms leading to formation and growth of  $C_n$  aggregates can only be done once the properties of the smaller ones have been clarified [6]. However, the existence of nearly isoenergetic isomers, a high-density of low-lying singlet and triplet electronic states, and a significant multi-reference character, makes their study theoretically most challenging [8,9].

Density functional theory (DFT) is the leading first-principles method used in computing electronic structure

and properties of medium and large-sized molecules, with Kohn–Sham [11] (KS) DFT being its mainstream. It offers an exact formulation of quantum mechanical electronic structure theory but relies on approximate exchange-correlation functionals [12]. This led to a proliferation of DFT functionals, with the best for one application being often not the best for another [13]. Recently [14], we have shown that second-order Möller–Plesset perturbation theoretic results extrapolated from the first steps of the hierarchical staircase to the complete basis set limit [15–17], MP2/CBS( $d, t$ ), can rival DFT/M06-2X ([12], and references therein) both on time and accuracy. Such a finding extends to other popular functionals: MP2/CBS( $d, t$ ) outperforms DFT/B3LYP-D3 [18] for the same cc-pVXZ (VXZ for brevity) basis set by showing energy errors at least twice smaller for the same reaction test set. In this work, we test the approach on the carbon clusters but consider DFT/MO6-2X only for  $C_4$  and  $C_8$  since there has recently been a study on  $C_n$  ( $n \leq 10$ ) using the same functional [19]. Suffice it to say that the trends reported elsewhere [14] are essentially maintained. Yet, as shown later, the MP2/CBS( $d, t$ ) energetics can still be enhanced at zero-cost to approximate couple-cluster quality via spin scaling [20], specifically using variable-scaling opposite spin [21] (VOS) theory.

## 2 Intermediate states: automated location

Of key importance, particularly in reaction dynamics, is the definition of a reaction path (as well as any underlying

<sup>\*</sup> Contribution to the Topical Issue “Atomic Cluster Collisions”, edited by Alexey Verkhovtsev, Andrey V. Solov'yov, Germán Rojas-Lorenzo, and Jesús Rubayo Soneira.

<sup>a</sup> e-mail: [varandas@uc.pt](mailto:varandas@uc.pt)

first-order saddle point or transition state [22]) that best represents a reactive process, an issue whose origin can be traced to the early stages of transition-state theory [23]. With various approaches implemented in electronic structure codes, one of the most useful bears on the concept of intrinsic reaction coordinate (IRC): a mass-weighted steepest descent path starting from a first-order saddle point [24] (and references therein). However, even prior to the appearance of the IRC concept, it emerged the idea of selecting a priori a coordinate to define the reaction path, with all other coordinates constrained or optimized in some manner. It turns out that the use of this driving coordinate approach may not be free from some ambiguity: the results may depend upon the choice of coordinates or even vary upon the sense of which direction the calculation progresses [25], and some paths so generated may give rise to discontinuities [26] and even not go through the saddle point for reaction. Still, the approach is simple to apply and useful if a well defined reaction coordinate is available, an issue further discussed along the text. Of particular relevance is the so-called optimum reaction coordinate [27,28] (ORC) path where all but the reactive coordinate (also called inactive) are optimized. Of course, likewise IRC, the ORC path may be forced to encompass a known stationary point, such as a transition state that connects two consecutive minima.

Due to the huge computational effort that is involved, the surge of DFT methods in computational chemistry comes with no surprise, particularly in fields like cluster chemistry and organometallic catalysis to find the many existing stationary points and even reaction pathways. Although chemical intuition and comparison with similar reactions can help on the endeavour, the number of such topographical features makes it a formidable task which, most importantly, remains prone to overlooks. To overcome drawbacks, the development of automated procedures to find intermediate species is pivotal. Although the use of fully automated methods has until recently been limited to unimolecular reactions in small systems [29–32], other tools for automated use aimed at larger systems: artificial force induced reaction [33], basin-hopping sampling [34], graph-based sampling [35], ab initio nanoreactor for discovering molecular species and the reactions between them and then automatically refining reaction paths [36], and transition state search using chemical dynamics simulations [37–39]. Some of these techniques combine geometrical approaches to identify the stationary point with dynamics simulations, with the minima obtained by tracing the intrinsic reaction coordinate paths from the transition states. With no claim at this stage of a fully elaborated tool, we suggest a simple scheme based solely on electronic structure calculations that should be able to locate the most relevant intermediates. The goal consists of inducing an adiabatic breakup of a bond (preferably at a minimum) which is then stimulated to discover one or more minima until fragmentation occurs. For clarity, we distinguish the present generalization of our previous ORC approach by referring it as optimized reaction coordinate for stimulated evolution (ORCSE), since it does not necessarily imply a single reaction and may

involve in principle any composite coordinate to achieve the desired evolution.

### 3 CBS extrapolation and reaction path

Clearly, any comparison of ab initio calculations with experimental data should at least consider extrapolation of the calculated property to the CBS limit [15–17,40–43]. This implies to split the total energy into Hartree–Fock (HF) and correlation (cor) components, since they obey distinct extrapolation laws [17]. Calculations of the HF and cor energy will then be carried out for all systems and geometries using for simplicity the smallest VXZ basis sets of Dunning [44,45]. Except if specified otherwise, core correlation effects are ignored. Two basic steps are then involved. Firstly, the most stable equilibrium geometries are characterized using MP2/VXZ calculations. The second step consists of single-point MP2 and CCSD(T) calculations plus CBS( $d, t$ ) extrapolations along the ORCSE path where all other degrees of freedom (DOF) are optimized. Corresponding M06-2X/VXZ calculations are also done but only for  $C_4$  and  $C_8$ .

The prediction of an accurate bond-breaking reaction path is nontrivial, particularly when aiming to visit all distinct (permutational equivalency aside) reaction intermediates. In the ORCSE method here suggested, the following three-point premise is accepted: (1) all intermediates are well approximated at MP2/CBS( $d, t$ ) level of theory; (2) all are accessible through a reaction coordinate that involves the stretch of a bond, a twist, or even a specially designed combination of stretches and twists, once all other DOF are fully optimized; (3) given the limitations of the optimization process, other paths may be potentially useful in unveiling other (unknown) stationary points. Although full optimization of all DOF but the inactive coordinate should in principle warrant completeness, this cannot be ensured due to difficulties in covering the full configuration space and the fact that most algorithms converge to the closest stationary point. Recall that some structures may be so totally unexpected that it is hardly conceivable whether any is missing, with the carbon clusters standing as paradigmatic examples.

### 4 The carbon clusters: results and discussion

Carbon clusters in the small size range have been described in many mass spectrometry experiments [1,2,46–53], and we focus on those involving between 4 and 10 C atoms. Known to have parallel sets of singlet and triplet forms, only the former are here considered. Both spin states have been extensively studied theoretically with high level electronic structure [1–3,54–59] and DFT [60,61] calculations, to mention just a brief list from where some results are used for comparisons.

The calculations here reported entail two parts. The first aims at validation of the method by testing its reliability on singlet  $C_4$  which we have studied elsewhere at high levels of ab initio theory [9]. For this, we consider the conversion of rhombic ( $r - C_4$ ) into linear ( $\ell - C_4$ ) isomeric

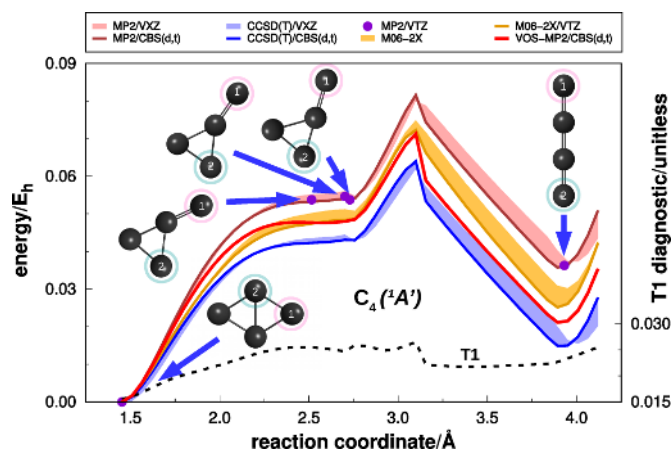


**Fig. 1.** ORCSE path showing all structural isomers of  $C_4(^1A')$  obtained by varying the distance between atoms 1 (circled in pink) and 2 (cyan). With  $R_{12}$  the inactive coordinate, all other DOF have been fully optimized, and the energies taken relative to the starting geometry. Where shown, in this and following plots, the shaded areas indicate the range of energies covered from  $DZ$  to  $CBS(d,t)$ , with the latter indicated by the solid colored line. A similar procedure is adopted for DFT, except for the line that refers now to  $M06-2X/VTZ$ . The dots indicate fully optimized  $MP2/VTZ$  energies, and the black dashed line the T1 diagnostic. For illustration purposes, two other structures (not necessarily stationary points up to a tight convergence) before and after the  $C_{2v}$  TS, are also shown.

structures as illustrated in Figure 1. Being the smallest cluster, the  $VTZ$  basis set is utilized [44,62], with all raw energies CBS extrapolated from the two lowest steps of the hierarchical staircase,  $x = d : D : 2$  and  $t : T : 3$ . All calculations were done with MOLPRO and the NOSYM command, thus warranting any expected symmetry only up to the numerical approximation used to locate the stationary points: this varied from threshold ( $\approx 10^{-4} E_h$ ) down to  $10^{-7} E_h$  accuracy.

Regarding  $C_4$ , previous theoretical work has identified the linear triplet and the cyclic (rhombic) singlet structures to lie close in energy: the former has been characterized spectroscopically, while the cyclic  $^1A_g$  form has thus far eluded positive identification. Figure 1 shows the ORCSE path for  $C_4(^1A')$  which, allowing for reliability checks, contains the full set of isomeric structures. The overall evolution process occurs in a plane and step-wise: starting from the  $^1A_g$  global minimum (rhombic), the system attains a  $C_s$  monocyclic ring form (distorted kite) via a ring-opening process in which a single peripheral bond is broken, crosses the  $C_{2v}$  transition state (TS), visits the other equivalent kite structure, and finally attains linearity after passing a peak of high energy associated with a  $L$ -shaped structure; see Figure 2. Along the ORCSE path, single-point  $MP2/VDZ$ ,  $VOS-MP2/VXZ$ , and  $CCSD(T)/VXZ$  ( $X = D, T$ ) calculations were also performed, with the raw energies subsequently  $CBS(d,t)$  extrapolated. The relevant numerical details are gathered in Table 1. Notably, the height of the  $C_{2v}$  transition state in  $C_4$  is predicted in remarkable agreement with our own best estimate [9] of  $29.73 \text{ kcal mol}^{-1}$

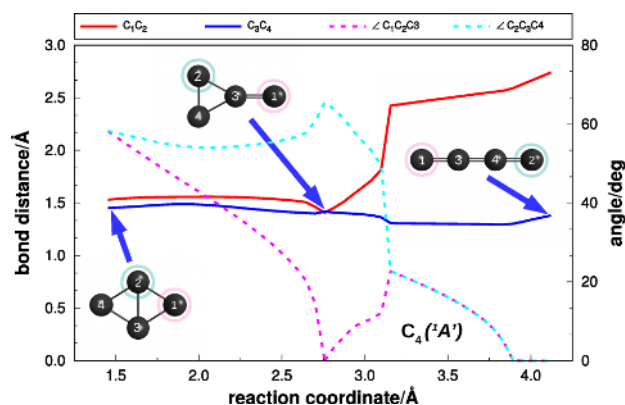


**Fig. 2.** Configurational DOF along the ORCSE path. Shown by the solid lines are the bond distances between atoms 2–3, and 3–4; the angles  $\angle 123$  and  $\angle 234$  are in dashed and refer to the right-hand-side axis. The dihedral angle is 180 deg over the whole evolution path.

at  $CASDC/CBS(T,Q)$  level using  $AVXZ$  basis sets, thus including both nondynamical and dynamical correlations at a level as high as possible (see Ref. [63] for the  $CASDC$  method). In turn, using  $M06-2X$  with a  $VDZ$  basis, the predicted value is  $33.1 \text{ kcal mol}^{-1}$ , hence similar to the corresponding  $MP2/CBS(d,t)$  of  $33.9 \text{ kcal mol}^{-1}$  here obtained. No comparison is possible with a  $VTZ$  basis, since  $M06-2X$  does not predict such a saddle point; a similar finding is reported by Ngandjong et al. [19] with  $M06-2X/AVDZ$ . Of course, the above remarkable agreement may have been somewhat accidental as the  $CASDC/CBS(T,Q)$  estimate [9] for the relative stability of the cyclic vs linear forms places the latter only  $6.14 \text{ kcal mol}^{-1}$  above the former, a value smaller by  $\sim 50\%$  than  $VOS-MP2/CBS(d,t)$  and nearly four times smaller than  $M06-2X$  [19].

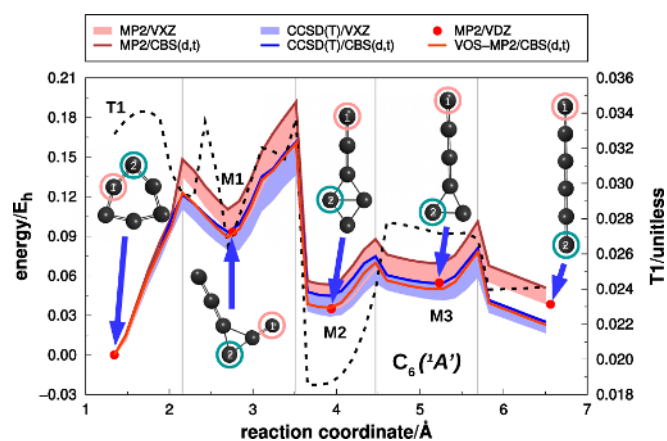
Also shown in Figure 1 is the T1 diagnostic for validity of the  $CCSD$  method: the accepted value at which it is no longer reliable is 0.02. Interestingly, the values along the ORCSE path are typically  $T1 < 0.025$ , thus suggesting that the nondynamical correlation may be less important than the dynamical, and hence that a restricted HF reference wavefunction should be reliable. Expectedly, in all cases the reported T1 values tend to peak at regions of instability, where the CC estimates are likely to be less reliable. Interestingly, while  $CCSD(T)$  tends to fail at such regions,  $VOS-MP2$  often gives reasonable estimates there, a welcome asset of the latter. Overall,  $M06-2X$  shows a good level of accuracy, occasionally slightly outperforming  $MP2/CBS(d,t)$  versus  $CCSD(T)/CBS(d,t)$ . However, it is mostly outperformed by  $VOS-MP2/CBS(d,t)$  at zero additional cost.

The same approach has been applied to  $C_6$ ,  $C_8$ , and  $C_{10}$  which were extensively studied, in particular by Yousaf and Taylor [3] and Belau et al. [2] who have used expensive  $CCSD(T)$  calculations. Likewise  $C_4$ ,  $C_6$  has provoked much discussion and many investigations about isomeric structures. Suffice it to say that recent work established the cyclic  $D_{3h}$  species as the most stable. As shown in Table 1, we predict the lowest singlet linear state of

**Table 1.** Energy, in kcal mol<sup>-1</sup>, of the relevant stationary points along the ORCSE path at CBS(*d, t*) level of theory<sup>a</sup>.

Struct.	VOS-MP2				CCSD(T)			
	<i>n</i> = 4	6	8	10	4	6	8	10
Linear	13.3	15.1 <sup>c</sup> (15.8 <sup>d</sup> )	6.5	82.1 <sup>e</sup> (58.5 <sup>f</sup> )	9.2	9.3 (17.2 <sup>g</sup> )	5.4	69.9 (68.6 <sup>h</sup> )
M3 <sup>b</sup>		31.4				26.5		
M2 <sup>b</sup>		22.7				20.7		
M1 <sup>b</sup>		56.7	8.7			51.6	12.5	
TS <sup>i</sup>	30.1				27.0			
Cyclic <sup>j</sup>	0	0	0	0	0	0	0	0

**Notes.** <sup>(a)</sup>Except for C<sub>4</sub> where a VTZ basis set has been employed, all CBS extrapolations were carried out at tightly converged,  $(1 - 10) \times 10^{-7}$  E<sub>h</sub>, optimum VDZ geometries. <sup>(b)</sup>Minima; see the relevant plots. <sup>(c)</sup>Relative to C<sub>6</sub>(D<sub>3h</sub>); MP2/CBS(*d, t*) is 33.3 kcal mol<sup>-1</sup>. <sup>(d)</sup>Relative to C<sub>6</sub>(D<sub>6h</sub>); MP2/CBS(*d, t*) is 39.1 kcal mol<sup>-1</sup>. <sup>(e)</sup>Relative to C<sub>10</sub>(D<sub>5h</sub>); MP2/CBS(*d, t*) is 77.9 kcal mol<sup>-1</sup>. <sup>(f)</sup>Relative to C<sub>10</sub>(D<sub>10h</sub>); MP2/CBS(*d, t*) is 118.5 kcal mol<sup>-1</sup>. <sup>(g)</sup>Relative to C<sub>10</sub>(D<sub>5h</sub>). <sup>(h)</sup>Relative to C<sub>10</sub>(D<sub>10h</sub>). <sup>(i)</sup>C<sub>2v</sub> saddle point in Figure 1. <sup>(j)</sup>Reference energies (from left to right): -151.82201053, -227.86923535, -303.91201521, -379.95203472, -151.84701142, -227.90334968, -303.95467509, and -380.00322690 E<sub>h</sub>.

**Fig. 3.** As in Figure 1 but for C<sub>6</sub>(<sup>1</sup>A').

C<sub>6</sub> to lie 15.8 kcal mol<sup>-1</sup> above the cyclic form, a value 2.5 kcal mol<sup>-1</sup> larger than for C<sub>4</sub> and not too far from existing DFT predictions [19]. It also compares well with earlier CCSD(T)/VDZ estimates [56] which cover the range between 7.1 and 18.4 kcal mol<sup>-1</sup>. As illustrated in Figure 3, the ORCSE path is more complicated than in C<sub>4</sub> but likewise the latter has been obtained uninterruptedly through a single run of optimizations which consisted of about 50 shots at MP2/VDZ level, and paralleled by single-point MP2, VOS-MP2, and CCSD(T) calculations with VXZ (*X* = D, T) bases, and finally CBS(*d, t*) extrapolated. Over much of the ORCSE path, T1 is sufficiently small to suggest that the SR calculations here reported should be reliable.

Similar to other even-numbered carbon clusters, C<sub>8</sub> is known to adopt both linear and cyclic structures as the most stable, with the cyclic isomer generally regarded to be more stable than the linear <sup>3</sup>Σ<sub>g</sub><sup>-</sup> species. Matrix isolation spectroscopy has found spectra assignable to both isomeric forms [64–70], while the linear species [69] has been detected by gas-phase electronic spectroscopy. Annealing experiments established that the cyclic species was the most stable [70]. Regarding the singlet states,

Table 1 shows that we predict the energy of linear C<sub>8</sub> to lie only about 6 kcal mol<sup>-1</sup> above the cyclic form at VOS-MP2 level, a value smaller than for C<sub>4</sub> and C<sub>6</sub> that agrees nicely with our own (see Tab. 1) as well as previous CCSD(T) estimates [56] of (4.1–15.3) kcal mol<sup>-1</sup> while being also in fair agreement with the M06-2X prediction [19]. It turns out that the cyclic C<sub>8</sub> structure predicted at MP2/VDZ level is not planar. In this regard, we should recall that floppy systems when calculated with a given basis may lead to the prediction of minima (saddle points) rather than saddle points (minima) when employing default convergence parameters, although they actually are true minima (saddle points) upon a tight convergence. Similar occurrences may turn out with changes of basis set. This is the case for cyclic C<sub>8</sub> which has symmetry C<sub>4h</sub> (<sup>1</sup>A<sub>g</sub>) with MP2/VTZ and CCSD(T)/VTZ but only C<sub>1</sub> with MP2/VDZ (the planar species shows as a saddle point of index 2). While an alert, this is not a limiting factor here, with all calculations along the ORCSE path done with the VDZ basis (except C<sub>4</sub>, done with VTZ) and threshold accuracy. Indeed, such a simplified approach is only used to predict the stationary points which can be next converged to the desired accuracy. MP2/VTZ, as well as CCSD(T) with both VDZ and VTZ, calculations have been subsequently carried out along the ORCSE path, and so have been the DFT/M06-2X ones here reported. Conversely to C<sub>4</sub>, Figure 4 shows that the latter are more insensitive to the basis set, while slightly outperforming MP2/CBS(*d, t*) along part of the path. However, they are almost always outperformed by VOS-MP2/CBS(*d, t*) at no additional cost.

Adaptations of the tool here reported for locating isomers of a given molecular formula suggest themselves for other ventures. Firstly, if doubts exist about other minima not located during the ORCSE path, it immediately comes to mind restart the procedure from any point along the previous path, and even redefine the ORC, say by using an angle (as in C<sub>4</sub> [9]) rather than a bond distance. For example, in the unlike case of distinct minima with a common R<sub>12</sub> bond distance, the lowest stationary point in energy is likely to be the only one obtained, although

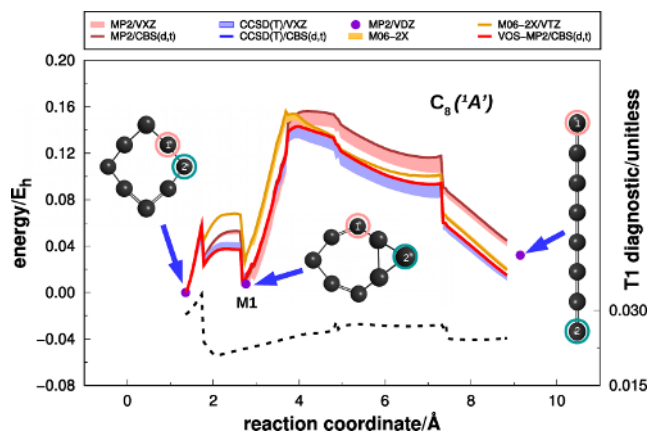


**Fig. 4.** As in Figure 1 but for  $C_8(^1A')$ . As the difference in size of the balls indicate, the structures depicted are non-planar: the cyclic is square-shaped but bent through a diagonal, M1 is a chair-type structure.

this cannot be warranted without using a global minimization search (itself of some inconvenience due to the possibility of introducing discontinuities in the ORCSE path). Additionally, in the case of equivalent minima, only one can be visited for a given value of  $R_{12}$ . This can be understood from the fact that every optimized geometry is uniquely defined for a specified value of the ORC, as it is seen for  $C_4$  from Figures 1 and 2; visiting another of such minima would then imply the use of an ORC distinct from  $R_{12}$ . The same would be expected if  $R_{12}$  were the common bond in both the double-ring  $C_{10}$  structure (two hexagons with a common side, the homologue of naphthalene) and the linear isomer. It turns out in this case that small double rings usually distort into monocyclic structures, and this is true for such a single state corresponding to the analog of naphthalene [57]. For a similar reason, one would not expect to get metastable structures. For example, the five-pointed star  $C_{10}$  could not be obtained, and this for an extra reason: it lies about 10 eV above the monocyclic structure [60], and still more than 3 eV above dissociation in  $C + C_9$  (see Fig. 5). Indeed, such structures may be of relevance in the study of carbon plasmas but are of little concern in chemical reaction dynamics where the methods here utilized hope to be realistic. Of course, one should add that the number and type of predicted stationary points depends on the method used, particularly at the DFT level. In fact, difficulties are expected with highly symmetric structures when a bond distance is selected for the inactive coordinate. A good example is  $C_8(O_h)$  which has been suggested from ab initio calculations to exist and even be regarded to have viability as an observable allotrope of carbon [71]. Besides lying much higher in energy than cyclic  $C_8$ , it appears impossible to attain it along the ORCSE path by simply cutting and stretching one bond. Instead, one obtains at MP2/VDZ level of theory a structure similar to number 3 in Figure 1 of reference [71], with the energy of the two highest-lying converged ORCSE points lying  $(42.5 \pm 2.4)$  kcal mol $^{-1}$  above  $C_8(O_h)$ . From these onwards, no optimizations could be done due to lack of

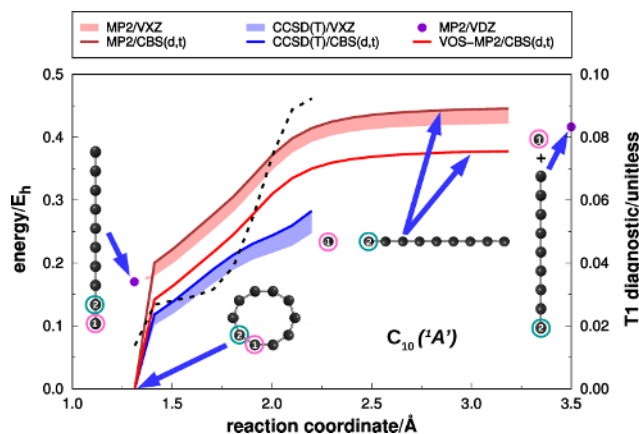


**Fig. 5.** As in Figure 1 but for  $C_{10}(^1A_1)$ , starting from the  $D_{10h}$  structure. The solid red dots are optimum energies of linear  $C_{10}$  and  $C + C_9$  products, with the latter indicated at  $R_{12} = 3.5$  Å, also at MP2/VDZ level of theory.

convergence of the HF orbitals. It turns out that our highest optimized point compares well in energy with the value 40.0 kcal mol $^{-1}$  encountered for the closest-in-shape stationary point at CCSD(T)/AVDZ level [71]. Clearly, we have adopted restricted HF in all calculations here reported, such as to avoid the problem of spin contamination but then convergence cannot be warranted at an arbitrary geometry. Of course, the possibility exists of searching for enhanced ORCs and optimization schemes at the unrestricted level, at least for exploratory work to define the ORCSE path: sections of this could then be attempted with restricted orbitals if so desired, a possibility not even attempted in the current work.

$C_{10}$  is recognized as a structural transition point for small neutral carbon clusters [64,65]. Although the linear structures are predicted close in energy to the cyclic ones for smaller clusters, the cyclic become more stable from  $C_{10}$  onwards [64,65]. Because  $C_{10}$  satisfies Hückel's rule for aromaticity, this is believed to give it added stability [65]. As Table 1 and Figure 5 show, our computations predict the cyclic to be 70–80 kcal mol $^{-1}$  more stable than the linear forms, thence consistent with previous CCSD(T) [2,56,72] and DFT/M06-2X [19] results.

Notably, the cyclic structure blows up at the very first stages of the ORCSE path to yield the linear form, from where it does not deviate much toward dissociation into a carbon atom plus a nine-atom cluster. Although the spin-spatial Wigner–Witmer rules allow both products to be in singlet or triplet states,  $C(^1D) + C_9(^1\Sigma_g^+)$  is the one that fits best the calculated data. Note that the fully optimized linear form lies on the continuation of the calculated ORCSE path to small  $R_{12}$  values. Indeed, we are not aware of any other stable structures of singlet  $C_{10}$  below dissociation that are predicted at the MP2 level of theory. Furthermore, Figure 5 shows that VOS-MP2/CBS( $d,t$ ) offers a generous estimate of the CCSD(T)/CBS( $d,t$ ) curve even when T1 attains huge values. A final remark on cyclic  $C_{10}$  which may adopt  $D_{5h}$  and  $D_{10h}$  closed-shell structures; the former shows good convergence (even

beyond threshold) to the minimum and 24 positive force constants, but fails to be well converged in the gradient norm (also converged in  $D_{10h}$ ). In fact, when the optimization is started in cartesian coordinates from the  $D_{5h}$  geometry, one is led to the  $D_{10h}$  minimum within  $10^{-7} E_h$ . As noted by Watts and Bartlett [54], the appetite of MP2 to predict the most stable structure to assume  $D_{10h}$  symmetry may be due to the need for “infinite-order” satisfied by the CC methods, a reason extensive to  $C_6$  in favoring  $D_{6h}$  versus  $D_{3h}$ . Indeed, CCSD(T) favors [54,56]  $D_{5h}$  by 2.9 (VDZ) and  $(1.0 \pm 0.1)$  kcal mol $^{-1}$  (VTZ), while our CBS( $d, t$ ) estimate does so by 1.3 kcal mol $^{-1}$ . Note that some larger energy differences in Table 1 are common in the literature [3,54]. The high values of T1 in Figure 5 may also help to complicate the analysis. Suffice to remark that: (i) the difference between the MP2/CBS( $d, t$ ) and CCSD(T)/CBS( $d, t$ ) energies may be partly ascribed to amplitudes that contribute to MP2 but not to CCSD(T), in a number expected to increase with cluster size; (ii) VOS enhances the agreement between the MP2 and CCSD(T) energies.

## 5 Concluding remarks

The reported results allow to glimpse in a 1D view all structures and energies of the even-numbered carbon clusters containing from 4 up to 10 atoms when they evolve from their cyclic to linear forms. Sequenced according to a pre-specified inactive coordinate that defines the ORCSE path, all structures (some possibly not yet reported but likely to be of interest in studying carbon plasmas) get naturally ordered and not randomly enumerated as often met in the literature. Done in an automated way, the method avoids common tedious work of guessing and optimizing such structures one at a time, a process that can only get more cumbersome with increasing size. Orbital-based, it still rivals DFT both in time and accuracy. In accordance with existing data for the singlets, the lowest energy structures are found to be cyclic. Because all optimized DOF become available along the ORCSE path, the task of locating saddle points [30] gets alleviated. If desired, optimizations along the ORCSE path can be constrained to a chosen set of DOF. Clearly, even in CCSD(T), the raw energies are not converged with respect to electron correlation. Yet, most of the error (expectedly down to a few tenths of a kcal mol $^{-1}$ ) from basis set incompleteness is hopefully recovered, a task hardly possible in a puristic ab initio way for the larger clusters. Notably, VOS-MP2/CBS( $d, t$ ) mimics well CCSD(T)/CBS( $d, t$ ) calculations, a significant result having in mind that the former can be done at the cost of a DFT calculation [14], thence at least one order of magnitude faster. Preliminary calculations on  $C_{12}$  and  $C_{16}$  have shown an equal efficiency, although it should be emphasized that in all cases the reliability of the predicted structures depends solely on the methodology, basis set, and balance achieved in describing nondynamical versus dynamical correlation, the limiting issues [3] to the topic here discussed. Finally, it should be recalled that rather than employing restricted orbitals, the approach here

suggested may employ (within their known limitations) unrestricted orbitals.

This work is supported by Fundação para a Ciência e a Tecnologia, Portugal. The support from COST Action CM1405 is also acknowledged.

## References

1. S. Arulmozhiraja, T. Ohno, J. Chem. Phys. **128**, 114301 (2008)
2. L. Belau, S.E. Wheeler, B.W. Ticknor, M. Ahmed, S.R. Leone, W.D. Allen, H.F. Schaefer III, M.A. Duncan, J. Am. Chem. Soc. **129**, 10229 (2007)
3. K.E. Yousaf, P.R. Taylor, Chem. Phys. **349**, 58 (2008)
4. N. Sakai, S. Yamamoto, Chem. Rev. **113**, 8981 (2013)
5. N.L.J. Cox, F. Patat, ApJ **565**, A61 (2014)
6. T.W. Yen, S.K. Lai, J. Chem. Phys. **142**, 084313 (2015)
7. S.K. Lai, I. Setiyawati, T.W. Yen, Y.H. Tang, Theor. Chem. Acc. **136**, 20 (2016)
8. C.M.R. Rocha, A.J.C. Varandas, J. Chem. Phys. **144**, 064309 (2016)
9. A.J.C. Varandas, C.M.M. Rocha, Philos. Trans. Roy. Soc. A **376**, 20170145 (2017)
10. S. Shaik, D. Danovich, W. Wu, P. Su, H.S. Rzepa, P.C. Hiberty, Nat. Chem. **4**, 195 (2012)
11. W. Kohn, L. Sham, Phys. Rev. A **140**, 1133 (1965)
12. R. Peverati, D.G. Truhlar, Phil. Trans. R. Soc. A **372**, 20120476 (2014)
13. N. Mardirossian, M. Head-Gordon, J. Chem. Theory Comput. **12**, 4303 (2016)
14. A.J.C. Varandas, M.M. González, L.A. Montero-Cabrera, J.M.G. de la Vega., Chem. Eur. J. **23**, 9122 (2017)
15. A.J.C. Varandas F.N.N. Pansini, J. Chem. Phys. **141**, 224113 (2014)
16. F.N.N. Pansini, A.C. Neto, A.J.C. Varandas, Theor. Chem. Acc. **135**, 261 (2016)
17. A.J.C. Varandas, Ann. Rev. Phys. Chem. **69**, 7.1 (2018)
18. S. Grimme, J. Comp. Chem. **27**, 1787 (2006)
19. A. Ngandjong, J. Mezei, J. Mougenot, A. Michau, K. Hassouni, G. Lombardi, M. Seydou, F. Maurel, Comp. Theor. Chem. **1102**, 105 (2017)
20. S. Grimme, J. Chem. Phys. **118**, 9095 (2006)
21. A.J.C. Varandas, J. Chem. Phys. **133**, 064104 (2010)
22. J.N. Murrell, K.J. Laidler, J. Chem. Soc. Faraday Trans. **64**, 371 (1968)
23. S. Glasstone, K. Laidler, H. Eyring, *The Theory of Rate Processes* (McGraw-Hill, New York, 1941)
24. S. Maeda, K. Morokuma, J. Chem. Theory Comput. **7**, 2335 (2011)
25. K. Ishida, K. Morokuma, A. Komornicki, J. Chem. Phys. **66**, 2153 (1977)
26. M.J.S. Dewar, S. Kirschner, J. Am. Chem. Soc. **93**, 4290 (1971)
27. A.J.C. Varandas, J. Phys. Chem. A **114**, 8505 (2010)
28. A.J.C. Varandas, Phys. Chem. Chem. Phys. **16**, 16997 (2014)
29. K. Bondensgard, F. Jensen, J. Chem. Phys. **104**, 8025 (1996)
30. W. Quapp, M. Hirsch, O. Imig, D. Heidrich, J. Comp. Chem. **19**, 1087 (1998)
31. K. Irikura, R. Johnson, J. Phys. Chem. A **104**, 2191 (2000)

32. E. Muller, A. de Meijere, H. Grubmuller, *J. Chem. Phys.* **116**, 897 (2002)
33. S. Maeda, S. Komagawa, M. Uchiyama, K. Morokuma, *Angew. Chem. Int. Ed.* **50**, 644 (2011)
34. D.J. Wales, J.P.K. Doye, *J. Phys. Chem. A* **101**, 5111 (1997)
35. S. Habershon, *J. Chem. Theor. Comput.* **12**, 1786 (2016)
36. L.-P. Wang, A. Titov, R. McGibbon, F. Liu, V.S. Pande, T.J. Martínez, *Nat. Chem.* **6**, 1044 (2014)
37. E. Martínez-Núñez, *Phys. Chem. Chem. Phys.* **17**, 14912 (2015)
38. E. Martínez-Núñez, *J. Comput. Chem.* **36**, 222 (2015)
39. J.A. Varela, S.A. Vázquez, E. Martínez-Núñez, *Chem. Sci.* **8**, 3843 (2017)
40. T. Helgaker, P. Jorgensen, J. Olsen, *Molecular Electronic-Structure Theory* (Wiley, Chichester, 2000)
41. W. Klopper, *Mol. Phys.* **6**, 481 (2001)
42. D.W. Schwenke, *J. Chem. Phys.* **122**, 014107 (2005)
43. A.J.C. Varandas, *J. Chem. Phys.* **126**, 244105 (2007)
44. T.H. Dunning Jr., *J. Chem. Phys.* **90**, 1007 (1989)
45. T.H. Dunning Jr., K.A. Peterson, D.E. Woon, in *Encyclopedia of Computational Chemistry*, edited by P.V.R. Schleyer, N.L. Allinger, T. Clark, J. Gasteiger, P.A. Kolman, H.F. Schaefer III (Wiley, Chichester, 1998), p. 88
46. E.A. Rohlfing, D.M. Cox, A. Kaldor, *J. Chem. Phys.* **81**, 3322 (1984)
47. H.W. Kroto, J.R. Heath, S.C. O'Brien, R.F. Curl, R.E. Smalley, *Nature* **318**, 162 (1985)
48. M.Y. Hahn, E.C. Honea, A.J. Paguia, K.E. Schriver, A.M. Camarena, R.L. Whetten, *Chem. Phys. Lett.* **130**, 12 (1986)
49. E.A. Rohlfing, *J. Chem. Phys.* **93**, 7851 (1990)
50. T. Moriwaki, K. Kobayashi, M. Osaka, M. Ohara, H. Shiromaru, Y. Achiba, *J. Chem. Phys.* **107**, 8927 (1997)
51. Y.K. Choi, H.S. Im, K.K.W. Jung, *Int. J. Mass Spectrom.* **189**, 115 (1999)
52. M.E. Geusic, M.F. Jarrold, T.J. McIlrath, R.R. Freeman, W.L. Brown, *J. Chem. Phys.* **86**, 3862 (1987)
53. C.H. Bae, S.M. Park, *J. Chem. Phys.* **117**, 5347 (2002)
54. J.D. Watts, R.J. Bartlett, *Chem. Phys. Lett.* **190**, 19 (1992)
55. J. Hutter, H.P. Lüthi, *J. Chem. Phys.* **101**, 2213 (1994)
56. J.M.L. Martin, P.R. Taylor, *J. Phys. Chem.* **100**, 6047 (1996)
57. R.O. Jones, *J. Chem. Phys.* **110**, 5189 (1999)
58. Y. Shlyakhter, S. Sokolova, A. Lüchow, J.B. Anderson, *J. Chem. Phys.* **110**, 10725 (1999)
59. A. Karton, A. Tarnopolsky, J.M. Martin, *Mol. Phys.* **107**, 977 (2009)
60. N.A. Poklonski, S.V. Ratkevich, S.A. Vyrko, *J. Phys. Chem. A* **119**, 9133 (2015)
61. C. Mauney, M.B. Nardelli, D. Lazzati, *ApJ* **800**, 30 (2015)
62. T.H. Dunning, K.A. Peterson, A.K. Wilson, *J. Chem. Phys.* **114**, 9244 (2001)
63. A.J.C. Varandas, *J. Chem. Chem. A* **117**, 7393 (2013)
64. W. Weltner Jr., R.J.V. Zee, *Chem. Rev.* **89**, 1713 (1989)
65. A.V. Orden, R.J. Saykally, *Chem. Rev.* **98**, 2313 (1998)
66. G. Monninger, M. Forderer, P. Gurtler, S. Kalhofer, S. Petersen, L. Nemes, P.G. Szalay, W. Kratschmer, *J. Phys. Chem. A* **106**, 5779 (2002)
67. J.D. Presilla-Marquez, J. Harper, J.A. Sheehy, P.G. Carrick, C.W. Larson, *Chem. Phys. Lett.* **300**, 719 (1999)
68. L. Lapinski, M. Vala, *Chem. Phys. Lett.* **300**, 195 (1999)
69. A.E. Boguslavskiy, J.P. Maier, *Phys. Chem. Chem. Phys.* **9**, 127 (2007)
70. N.G. Gotts, G. von Helden, M.T. Bowers, *Int. J. Mass Spectrometry Ion Process.* **149/150**, 217 (1995)
71. D. Sharapa, A. Hirsch, B. Meyer, T. Clark, *Chem. Phys. Chem.* **16**, 2165 (2015)
72. V. Parasuk, J. Almlöf, *Theor. Chim. Acta.* **83**, 227 (1992)